PLOS ONE

RESEARCH ARTICLE

The complete mitochondrial genome of *Calyptogena marissinica* (Heterodonta: Veneroida: Vesicomyidae): Insight into the deep-sea adaptive evolution of vesicomyids

Mei Yang[1,2,3,4], **Lin Gong**[1,2,3,4], **Jixing Sui**[1,2,3,4], **Xinzheng Li**[1,2,3,4]*

1 Department of Marine Organism Taxonomy and Phylogeny, Institute of Oceanology, Chinese Academy of Sciences, Qingdao, China, **2** Center for Ocean Mega-Science, Chinese Academy of Sciences, Qingdao, China, **3** Laboratory for Marine Biology and Biotechnology, Qingdao National Laboratory for Marine Science and Technology, Qingdao, China, **4** University of Chinese Academy of Sciences, Beijing, China

* lixzh@qdio.ac.cn

Citation: Yang M, Gong L, Sui J, Li X (2019) The complete mitochondrial genome of *Calyptogena marissinica* (Heterodonta: Veneroida: Vesicomyidae): Insight into the deep-sea adaptive evolution of vesicomyids. PLoS ONE 14(9): e0217952. https://doi.org/10.1371/journal.pone.0217952

Editor: Marc Robinson-Rechavi, Universite de Lausanne Faculte de biologie et medecine, SWITZERLAND

Received: May 21, 2019

Accepted: August 23, 2019

Published: September 19, 2019

Data Availability Statement: All complete sequences of Calyptogena marissinica mitochondrial genome files are available from the GenBank database (accession number: MK948426).

Funding: This research was funded by the National Key R&D Program of China, 2018YFC0309804 to LG, the National Natural Science Foundation of China, 41506173 to MY, and Strategic Priority

Abstract

The deep-sea chemosynthetic environment is one of the most extreme environments on the Earth, with low oxygen, high hydrostatic pressure and high levels of toxic substances. Species of the family Vesicomyidae are among the dominant chemosymbiotic bivalves found in this harsh habitat. Mitochondria play a vital role in oxygen usage and energy metabolism; thus, they may be under selection during the adaptive evolution of deep-sea vesicomyids. In this study, the mitochondrial genome (mitogenome) of the vesicomyid bivalve *Calyptogena marissinica* was sequenced with Illumina sequencing. The mitogenome of *C. marissinica* is 17,374 bp in length and contains 13 protein-coding genes, 2 ribosomal RNA genes (*rrnS* and *rrnL*) and 22 transfer RNA genes. All of these genes are encoded on the heavy strand. Some special elements, such as tandem repeat sequences, "$G(A)_nT$" motifs and AT-rich sequences, were observed in the control region of the *C. marissinica* mitogenome, which is involved in the regulation of replication and transcription of the mitogenome and may be helpful in adjusting the mitochondrial energy metabolism of organisms to adapt to the deep-sea chemosynthetic environment. The gene arrangement of protein-coding genes was identical to that of other sequenced vesicomyids. Phylogenetic analyses clustered *C. marissinica* with previously reported vesicomyid bivalves with high support values. Positive selection analysis revealed evidence of adaptive change in the mitogenome of Vesicomyidae. Ten potentially important adaptive residues were identified, which were located in *cox1*, *cox3*, *cob*, *nad2*, *nad4* and *nad5*. Overall, this study sheds light on the mitogenomic adaptation of vesicomyid bivalves that inhabit the deep-sea chemosynthetic environment.

Introduction

Mitochondria, which descended from Proteobacteria via endosymbiosis, are important organelles in eukaryotic cells and are involved in various processes, such as ATP generation,

Research Program of the Chinese Academy of Sciences, XDB06010101 to XL. The funders had no role in study design, data collection and analysis, decision to publish, or preparation of the manuscript.

Competing interests: The authors have declared that no competing interests exist.

signaling, cell differentiation, growth and apoptosis [1]. Moreover, mitochondria have their own genetic information system. In general, the metazoan mitogenome is a closed, circular DNA molecule, ranging from 12 to 20 kb in length and usually containing 37 genes: 13 protein-coding genes (PCGs) (*atp6*, *atp8*, *cox1-3*, *cob*, *nad1-6* and *nad4l*) of the respiratory chain, 2 ribosomal RNA (rRNA) genes (*rrnS* and *rrnL*) and 22 transfer RNA (tRNA) genes [2]. In addition, there are several noncoding regions in the mitogenome, and the longest noncoding "AT-rich" region is normally interpreted as the control region (CR), which includes elements controlling the initiation and regulation of transcription and replication [3]. Owing to variable gene order, a low frequency of gene recombination and different genes having different evolutionary rates, mitochondrial sequences are widely used for species identification, genetic diversity assessment and phylogenetics at various taxonomic levels [4–7].

Since the discovery of cold seeps and hydrothermal vents in the deep-sea, the unique biological communities that depend on chemosynthetic primary production have attracted the attention of researchers [8–11]. These deep-sea chemosynthetic environments lack sunlight and exhibit high pressure, low oxygen and high levels of chemical toxicity due to various heavy metals, and the organisms that live there show a series of adaptations (more complex innate immune system, expanded gene families for stabilizing protein structures and removing toxic substances, a set of positively selected genes related to cytoskeleton structures, DNA repair and genetic information processing) compared with marine species in coastal environments [12–15]. Mitochondria are the energy metabolism centers of eukaryotic cells, which can generate more than 95% of cellular energy through oxidative phosphorylation (OXPHOS) [3]. Therefore, mitochondrial PCGs may undergo evolutionary selection in response to metabolic requirements in extremely harsh environments [16–18]. Numerous studies have found clear and compelling evidence of adaptive evolution in the mitogenome of organisms from extreme habitats, including Tibetan humans [19], Chinese snub-nosed monkeys [20], Tibetan horses [21–22], Tibetan wild yaks [23], galliform birds [24], and Tibetan loaches [25].

The family Vesicomyidae (Dall & Simpson, 1901) is widely distributed worldwide from shelf to hadal depths and comprises specialized bivalves occurring in reducing environments such as hydrothermal vents located in mid-ocean ridges and back-arc basins, cold seeps at continental margins and whale falls [26–29]. Studies have shown that vesicomyid bivalves rely upon the symbiotic chemoautotrophic bacteria in their gills for all or part of nutrition [30–31]. Based on the shells and soft body, the Vesicomyidae is divided into two subfamilies: Vesicomyinae and Pliocardiinae. The Vesicomyinae includes only one genus, *Vesicomya*, while Pliocardiinae currently contains 20 genera. Among the 20 genera, *Calyptogena* is the most diverse group of deep-sea vesicomyid bivalves in the western Pacific region and its marginal seas [32]. As some of the dominant species in the deep-sea, vesicomyids are an interesting taxon with which to study the mechanisms of adaptation to diverse stressors in deep-sea habitats. Considering that the mitogenome has highly compact DNA and is easily accessible, several complete/nearly complete mitogenomes of vesicomyids have been sequenced [33–36] in recent years; however, limited information is available about the mechanism of adaptation to deep-sea habitats in vesicomyids at the mitogenome level.

In the present study, we obtained the mitogenome of *Calyptogena marissinica*, a new species of the family Vesicomyidae from the Haima cold seep of the South China Sea. First, the mitogenome organization, codon usage, and gene order information were obtained, and we compared the composition of this mitogenome with that of other available vesicomyid bivalve mitogenomes. Second, based on mitochondrial PCGs and 2 rRNA genes, the phylogenetic relationships between *C. marissinica* and other species from subclass Heterodonta were examined. Finally, to understand the adaptive evolution of deep-sea organisms, we conducted positive selection analysis of vesicomyid bivalve mitochondrial PCGs.

Materials and methods

Sampling, identification and DNA extraction

Specimen of *C. marissinica* was sampled from the "Haima" methane seep in the northern sector of the South China Sea, 16˚43.80′N, 110˚28.50′E, 1,390 m, using a remotely operated vehicle (ROV) in May 2018. Species-level morphological identification was performed according to the main points of Chen et al. (2018) [32]. Specimen was dissected and different tissues were preserved separately at -80˚C until DNA extraction. Total genomic DNA was extracted from the adductor muscle tissue using a DNeasy tissue kit (Qiagen, Beijing, China) following the manufacturer's protocols.

Illumina sequencing, mitogenome assembly and annotation

After DNA isolation, 1 μg of purified DNA was fragmented, used to construct short-insert libraries (insert size of 430 bp) according to the manufacturer's instructions (TruSeq™ Nano DNA Sample Prep Kit, Illumina), and then sequenced on an Illumina HiSeq 4000 instrument (San Diego, USA).

Prior to assembly, raw reads were filtered by Trimmomatic 0.35. This filtering step was performed to remove the reads with adaptors, the reads showing a quality score below 20 ($Q<20$), the reads containing a percentage of uncalled bases ("N" characters) equal to or greater than 10% and the duplicated sequences. The mitochondrial genome was reconstructed using a combination of *de novo* and reference-guided assemblies, and the following three steps were used to assemble the mitogenome. First, the filtered reads were assembled into contigs using SPAdes 3.10.1. Second, contigs were aligned to the reference mitogenomes from species of the family Vesicomyidae using BLAST (https://blast.ncbi.nlm.nih.gov/Blast.cgi), and aligned contigs ($\geq$80% similarity and query coverage) were ordered according to the reference mitogenomes. Third, clean reads were mapped to the assembled draft mitogenome using GapCloser 1.12 with default parameters, and the majority of gaps were filled via local assembly.

The mitochondrial genes were annotated using homology alignments and *de novo* prediction, and EVidenceModeler [37] was used to integrate the gene set. rRNA genes and tRNA genes were predicted by rRNAmmer [38] and tRNAscan-SE [39]. A whole-mitochondrial genome BLAST search (E-value $\leq 1e^{-5}$, minimal alignment length percentage $\geq$ 40%) was performed against 5 databases, namely, the KEGG (Kyoto Encyclopedia of Genes and Genomes), COG (Clusters of Orthologous Groups), NR (Non-Redundant Protein), Swiss-Prot and GO (Gene Ontology) databases. Organellar Genome DRAW [40] was used for circular display of the *C. marissinica* mitogenome.

Sequence analysis

The nucleotide composition and codon usage were computed using DnaSP 5.1 [41]. The AT and GC skews were calculated with the following formulas: AT skew = (A − T) / (A + T) and GC skew = (G − C) / (G + C) [42], where A, T, G and C are the occurrences of the four nucleotides. Tandem Repeats Finder 4.0 [43] was used to search for the tandem repeat sequences. The online version of Mfold [44] was applied to infer potential secondary structure, and if more than one secondary structure appeared, the one with the lowest free energy score was used.

Phylogenetic analysis

The phylogeny of the subclass Heterodonta was reconstructed using mitogenome data from 41 species, including 2 Lucinida species, 2 Myoida species, and 37 Veneroida species, and

Chlamys farreri and *Mimachlamys nobilis* from the subclass Pteriomorphia served as outgroups (S1 Table). Our data set was based on nucleotide and amino acid sequences from 9 mitochondrial PCGs (*cox1*, *cox2*, *cox3*, *cob*, *atp6*, *nad1*, *nad4*, *nad5*, and *nad6*) and 2 rRNA genes. The *atp8*, *nad2*, *nad4l* and *nad6* sequences were excluded due to several species with incomplete mitogenomes. Multiple alignments of the whole 11 genes were conducted using MUSCLE 3.8.31. In aligned sequences, ambiguously aligned regions and gaps were removed using Gblocks server 0.91b [45] with the default setting. ModelTest 2.1.10 [46] and ProtTest 3.4 [47] were used to select the best-fit evolutionary models GTR + I + G and LG + I + G + F for the nucleotide dataset and amino acid dataset, respectively. Maximum likelihood (ML) analysis was performed using RAxML 8.2.8 [48]. Topological robustness for the ML analysis was evaluated with 100 replicates of bootstrap support. Bayesian inference (BI) was conducted using MrBayes 3.2.6 [49], and four Markov chain Monte Carlo (MCMC) chains were run for 10^6 generations, with sampling every 100 generations and a 25% relative burn-in. All phylogenetic trees were graphically edited with the iTOL 3.4.3 (https://itol.embl.de/itol.cgi).

Positive selection analysis

Comparing the nonsynonymous/synonymous substitution ratios ($\omega = dN/dS$) has become a useful approach for quantifying the impact of natural selection on molecular evolution [50]. $\omega > 1$, $= 1$ and < 1 indicate positive selection, neutrality and purifying selection, respectively [51]. The codon-based maximum likelihood (CodeML) method implemented in the PAML package [52] was applied to estimate the dN/dS ratio ω. The combined database of 13 mitochondrial PCGs was used for the selection pressure analyses (S2 Table). Both the ML and Bayesian phylogenetic trees were separately used as the working topology in all CodeML analyses.

To evaluate positive selection in the vesicomyid bivalves, we used branch models in the present study. First, the one-ratio model (M_0) estimate the distribution of ω values as a benchmark under an assumption of no adaptive evolution in the gene sequences, which assumes a single ω ratio for all branches in the phylogeny [53]. Then, the two-ratio model (M_2), which allows the background lineages and foreground lineages to have different ω ratio values, was used to detect positive selection acting on branches of interest [54–55]. Last, a free-ratio model (M_1), which allows ω ratio variation among branches, was used to estimate ω values on each branch [55]. Here, the one-ratio model (M_0) and the free-ratio model (M_1) were compared to confirm whether different clades in Heterodonta had different ω values. Additionally, we compared the one-ratio model (M_0) and the two-ratio model (M_2) to investigate whether deep-sea vesicomyid clades are subjected to more selection pressure than other Heterodonta species in coastal waters. ω_0 and ω_1 represent the values for the other Heterodonta clades in the phylogeny and the vesicomyid clades, respectively. Pairwise models were compared with critical values of the Chi square (χ^2) distribution using likelihood ratio tests (LRTs), in which the test statistic was estimated as twice the difference in log likelihood ($2\Delta L$) and the degrees of freedom were estimated as the difference in the number of parameters for each model.

Furthermore, we fit branch-site models to examine positive selection on some sites among the vesicomyid clades. Branch-site models allow ω to vary both among sites in the protein and across branches on the tree. Branch-site model A (positive selection model) was used to identify the positively selected sites among the lineages of vesicomyids (marked as foreground lineages). The presence of sites with $\omega > 1$ suggests that model A fits the data significantly better than the corresponding null model. Bayes Empirical Bayes analysis was used to calculate posterior probabilities in order to identify sites under positive selection on the foreground lineages if the LRTs was significant [56].

Results and discussion

C. marissinica mitogenome organization

The Illumina HiSeq runs resulted in 20,359,890 paired-end reads from the *C. marissinica* library with an insert size of approximately 450 bp. Selective-assembly analysis showed that 312,068 reads were assembled into a 17,374 bp circular molecule, which represented the complete mitogenome of *C. marissinica* (Fig 1 and Table 1). This length is shorter than that of the complete mitogenome of other vesicomyid bivalves, which ranges from 19,738 bp in *Calyptogena magnifica* [33] to 19,424 bp in *Abyssogena phaseoliformis* [35]. The genome encodes 37 genes, including 13 PCGs, 2 rRNA genes, and 22 tRNA genes (duplication of $tRNA^{Leu}$ and $tRNA^{Ser}$). All of the genes are encoded on the heavy (H) strand, as consistently reported for other bivalves [35–36,56], and transcribed in the same direction. A total of 2,287 bp of noncoding nucleotides are scattered among 23 intergenic regions varying from 1 to 1,676 bp in length (Table 1). The largest noncoding region (1,676 bp) is located between $tRNA^{Trp}$ and *nad6* and is identified as the putative control region (CR) due to its location and high A+T content (73.3%). Furthermore, there are four overlaps between adjacent genes in the *C. marissinica* mitogenome with a size range of 1 to 5 bp ($tRNA^{Glu}$ / $tRNA^{Ser(UCA)}$, $tRNA^{Leu(UUA)}$ / *nad1*, *rrnS* / $tRNA^{Met}$, and *cox3* / $tRNA^{Phe}$).

The *C. marissinica* mitogenome has a nucleotide composition of 25.9% A, 10.8% C, 23.8% G, and 39.5% T and an overall AT content of 65.4%. The AT skew and GC skew are well conserved among vesicomyids, which vary from -0.165 to -0.230 and 0.343 to 0.440, respectively (Table 2). For the *C. marissinica* mitogenome, the AT skew is -0.209, and the GC skew is 0.375, which indicates bias toward T and G similar to that in other vesicomyids. The complete mitochondrial DNA sequence has been deposited in GenBank under accession number MK948426.

Protein-coding genes

The total length of all 13 PCGs of *C. marissinica* is 11,775 bp, accounting for 67.8% of the complete length of the mitogenome, and the PCGs encode 3,912 amino acids (Table 2). In the mitogenome of metazoans, most PCGs start with the standard ATN codon [2,57–58]. In the present study, with the exception of the *atp8* gene, which had the alternate initiation codon GTG, all the PCGs were initiated by typical ATN codons: 6 genes (*atp6*, *cob*, *cox1*, *cox2*, *cox3*, and *nad4*) were initiated by ATG, 4 genes (*nad2*, *nad3*, *nad4l*, and *nad6*) were initiated by ATT, and 2 genes (*nad1* and *nad5*) were initiated by ATA. Notably, genes are commonly initiated by GTG in vesicomyid bivalves [34], and the amino acid encoded by GTG is valine, which belongs to the nonpolar amino acids, such as methionine and isoleucine encoded by ATN. Moreover, in eight other vesicomyid bivalves (*Archivesica* sp., *Archivesica gigas*, *Archivesica pacifica*, *C. magnifica*, *Abyssogena mariana*, *Ab. phaseoliformis*, *Isorropodon fossajaponicum*, and *Phreagena okutanii*), *cox3* had a truncated termination codon, TA [34]. Previous studies have shown that the truncated stop codon is common in the metazoan mitogenome and might be corrected by posttranscriptional polyadenylation [59–60]. However, in the mitogenome of *C. marissinica*, all of the PCGs were ended by a complete TAA (*atp6*, *cob*, *cox1*, *cox2*, *nad3*, *nad4*, *nad4l*, *nad5*, and *nad6*) or TAG (*atp8*, *cox3*, *nad1*, and *nad2*) termination codon.

Numerous studies have indicated that metazoan mitogenomes usually have a bias toward a higher representation of nucleotides A and T, leading to a subsequent bias in the corresponding encoded amino acids [58,61–63]. In the mitogenome of *C. marissinica*, the A+T contents of PCGs and third codon positions are 63.2% and 69.7%, respectively, which are similar to the values observed in other vesicomyids (Table 2). The amino acid usage and relative

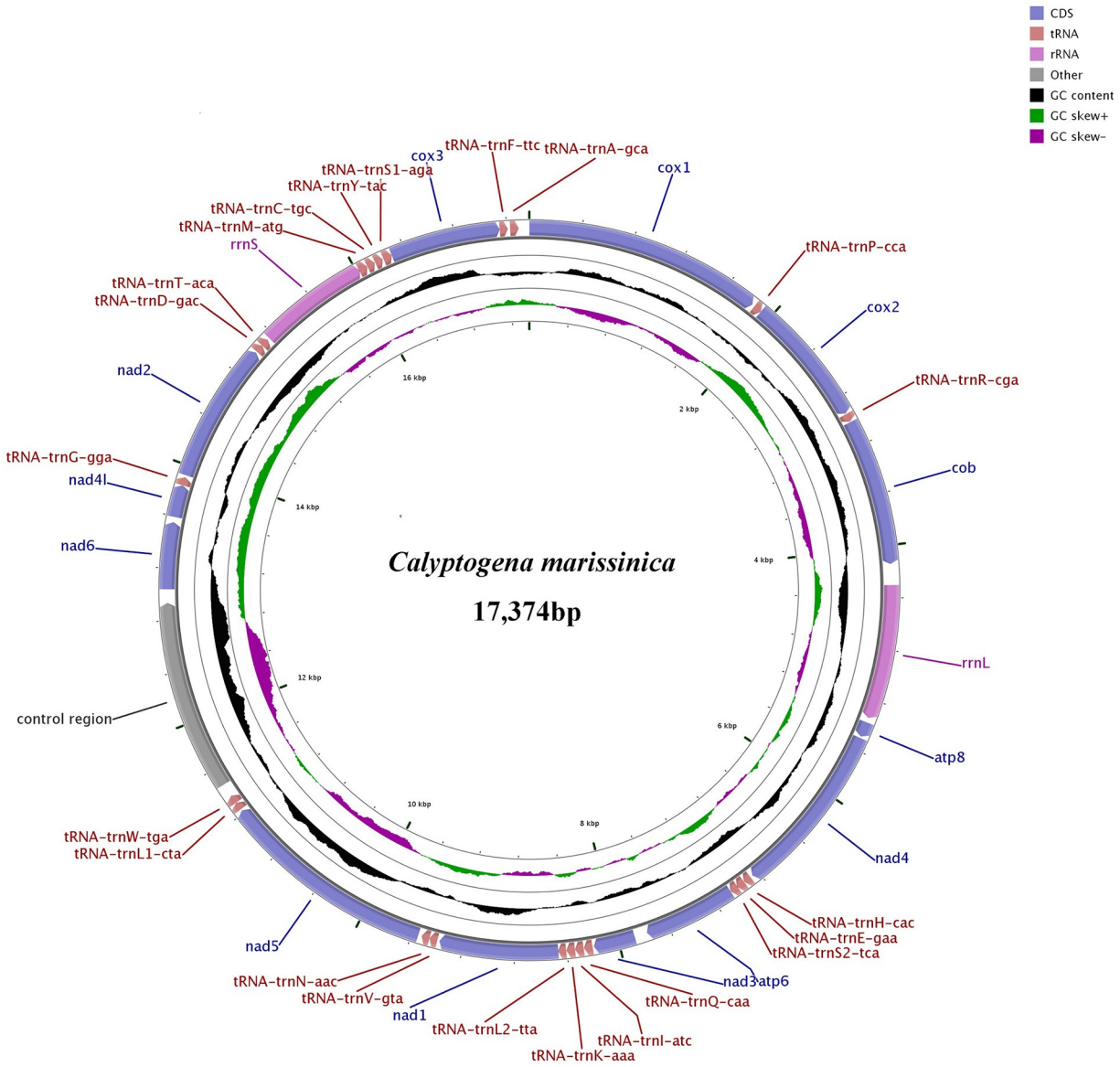

Fig 1. Complete mitogenome map of *C. marissinica*. All 37 genes are encoded on the heavy (H) strand. Genes for proteins and rRNAs are shown with standard abbreviations. Genes for tRNAs are displayed by a single letter for the corresponding amino acid, with two leucine tRNAs and two serine tRNAs differentiated by numerals.

https://doi.org/10.1371/journal.pone.0217952.g001

synonymous codon usage (RSCU) values in the PCGs of *C. marissinica* are summarized in Fig 2. The mitogenome encodes a total of 3,912 amino acids, among which leucine (13.6%) and glutamine (1.4%) are the most and the least frequently used, respectively. As mentioned earlier, the amino acids encoded by A+T-rich codon families (Asn, Ile, Lys, Met, Phe and Tyr) have a higher frequency of use than those encoded by G+C-rich codon families (Ala, Arg, Gly and Pro). The RSCU values indicate that the six most commonly used codons are TTA (Leu), ACT (Thr), GGG (Gly), TCT (Ser), GCT (Ala), and CCT (Pro) (Fig 2), which show A+T bias at their third codon position. In addition, the codons with A and T in the third position are used more frequently than other synonymous codons. These features reflect codon usage with A

Table 1. Mitogenome organization of *C. marissinica*.

Name	Strand	Range	Size		Codon			Intergenic nucleotides
			Nucleotides	Amino acids	Start	Stop	Anticodon	
cox1	+	1–1833	1833	610	ATG	TAA		-
tRNA-Pro	+	1854–1917	64				TGG	20
cox2	+	1918–2934	1017	338	ATG	TAA		0
tRNA-Arg	+	2941–3005	65				TCG	6
cob	+	3010–4143	1134	377	ATG	TAA		4
rrnL	+	4305–5340	1036					161
atp8	+	5377–5493	117	38	—	TAG		36
nad4	+	5506–6852	1347	448	ATG	TAA		12
tRNA-His	+	6873–6933	61				GTG	20
tRNA-Glu	+	6934–6999	66				TTC	0
tRNA-Ser^{UCA}	+	6996–7059	64				TGA	-4
atp6	+	7060–7773	714	237	ATG	TAA		0
nad3	+	7872–8192	321	106	ATT	TAA		98
tRNA-Gln	+	8203–8269	67				TTG	10
tRNA-Ile	+	8272–8338	67				GAT	2
tRNA-Lys	+	8339–8405	67				TTT	0
tRNA-Leu^{UUA}	+	8407–8469	63				TAA	1
nad1	+	8467–9381	915	304	ATA	TAG		-3
tRNA-Val	+	9399–9460	62				TAC	17
tRNA-Asn	+	9461–9522	62				GTT	0
nad5	+	9550–11223	1674	557	ATA	TAA		27
tRNA-Leu^{CUA}	+	11236–11297	62				TAG	12
tRNA-Trp	+	11298–11362	65				TCA	0
contral region	+	11363–13038	1676					0
nad6	+	13039–13554	516	171	ATT	TAA		0
nad4l	+	13595–13843	249	82	ATT	TAA		40
tRNA-Gly	+	13844–13907	64				TCC	0
nad2	+	13925–15010	1086	361	ATT	TAG		17
tRNA-Asp	+	15020–15081	62				GTC	9
tRNA-Thr	+	15082–15142	61				TGT	0
rrnS	+	15160–16027	868					17
tRNA-Met	+	16023–16089	67				CAT	-5
tRNA-Cys	+	16092–16153	62				GCA	2
tRNA-Tyr	+	16159–16220	62				GTA	5
tRNA-Ser^{AGA}	+	16228–16296	69				TCT	7
cox3	+	16297–17148	852	283	ATG	TAG		0
tRNA-Phe	+	17148–17210	63				GAA	-1
tRNA-Ala	+	17228–17293	66				TGC	17

https://doi.org/10.1371/journal.pone.0217952.t001

and T biases at the third codon position, which are similar to the biases that exist in many metazoans [16,64–66].

Ribosomal RNA and transfer RNA genes

The *rrnL* and *rrnS* genes of *C. marissinica* are 1,036 bp (AT% = 67.2) and 868 bp (AT% = 67.7) in length, respectively. As in other vesicomyid bivalves, *rrnL* is located between the *cob* and

Table 2. Mitogenomes of Vesicomyidae species sequenced to date and their genomic features.

Species	Genus	Accession number	Length (bp)	Genome			Protein-coding genes			*rrnL*		*rrnS*		tRNAs		Control region	
				AT %	AT skew	GC skew	Length (aa)	AT % (all)	AT% (3rd)	Length (bp)	AT %	Length (bp)	AT %	Number/ Length (bp)	AT %	Length (bp)	AT %
Abyssogena mariana[1]	*Abyssogena*	LC126311	15,927*	69.8	-0.210	0.408	3884	69.0	73.9	1196	71.2	862	70.8	23/1279	71.7	-	-
Abyssogena phaseoliformis	*Abyssogena*	AP014557	19,424	70.4	-0.199	0.440	3881	68.3	73.7	1196	71.2	862	70.9	24/1282	70.4	3,438	74.4
Akebiconcha kawamurai[2]	*Akebiconcha*	AP014551	12,946*	65.2	-0.222	0.371	3249	62.5	68.7	1194	69.7	205	67.7	17/1090	69.0	-	-
Archivesica gigas[1]	*Archivesica*	MF959623	15,674*	65.0	-0.228	0.389	3878	63.6	70.6	1223	68.9	879	67.9	21/1212	68.7	-	-
Archivesica pacifica[1]	*Archivesica*	MF959624	17,782*	68.6	-0.214	0.429	4002	67.1	79.5	1226	71.3	885	69.9	22/1282	69.6	-	-
Archivesica sp.[1]	*Archivesica*	MF959622	15,650*	64.8	-0.228	0.386	3889	63.7	70.8	1221	69.0	879	67.8	20/1214	68.7	-	-
Calyptogena fausta[2]	*Calyptogena*	AP014549	13,509*	66.0	-0.218	0.394	3410	0.64 64.7	70.7	1189	70.3	205	67.8	17/1092	70.0	-	-
Calyptogena laubirei[2]	*Calyptogena*	AP014553	12,968*	64.3	-0.226	0.361	3259	61.6	67.1	1191	69.0	204	67.2	17/1090	67.8	-	-
Calyptogena magnifica	*Calyptogena*	NC_028724	19,738	68.4	-0.195	0.390	3928	65.5	75.6	1219	70.5	935	70.0	22/1347	70.2	3,910	75.2
Calyptogena marissinica	*Calyptogena*	MK948426	17,374	65.4	-0.209	0.375	3912	63.2	69.7	1,036	67.2	868	67.7	22/1,411	68.7	1,676	73.3
Calyptogena nautilei[2]	*Calyptogena*	AP014554	13,281*	69.4	-0.196	0.353	3298	68.0	74.4	1182	72.1	204	72.1	17/1088	71.4	-	-
Calyptogena pacifica[2]	*Calyptogena*	AP014556	13,454*	67.6	-0.222	0.420	3390	66.6	72.6	1195	70.8	204	69.6	17/1088	69.5	-	-
Isorropodon fossajaponicum[1]	*Isorropodon*	AP014550	19,556*	68.2	-0.165	0.343	3894	66.6	70.6	1199	70.3	861	68.3	24/1290	70.3	-	-
Phreagena kilmeri[2]	*Phreagena*	AP014552	12,944*	64.9	-0.223	0.365	3249	63.4	68.0	1191	69.5	204	68.3	17/1089	68.7	-	-
Phreagena okutanii[1]	*Phreagena*	AP014555	16,336*	65.6	-0.230	0.405	3833	64.0	68.1	1191	69.7	861	67.7	23/1277	68.9	-	-
Phreagena soyoae[2]	*Phreagena*	AP014558	12,941*	64.9	-0.223	0.365	3249	63.4	67.9	1190	69.5	204	68.1	17/1089	68.7	-	-
Pliocardia stearnsii[2]	*Pliocardia*	AP014559	13,012*	67.7	-0.230	0.402	3265	66.6	72.7	1201	71.6	203	69.5	17/1096	69.1	-	-

Note:

*indicates incomplete mitogenomes.

[1] Incomplete mitogenomes for which the control region was not sequenced.

[2] Incomplete mitogenomes for which *nad2*, *nad4l*, *nad6*, a few tRNA genes and the control region were not sequenced.

https://doi.org/10.1371/journal.pone.0217952.t002

atp8 genes, and *rrnS* is located between $tRNA^{Thr}$ and $tRNA^{Met}$. The largest known *rrnL* and *rrnS* genes are 1,226 bp in *Ar. pacifica* and 935 bp in *C. magnifica*, respectively [33–35].

Twenty-two tRNA genes were identified in the mitogenome of *C. marissinica*, which is typical for metazoans. However, the number of tRNA genes varies among other vesicomyid bivalves (Table 2). The length of tRNA genes in *C. marissinica* ranges from 61 ($tRNA^{His}$ and $tRNA^{Thr}$) to 69 ($tRNA^{Ser\ (AGA)}$) bp (Table 1), and the AT content of the tRNA genes is 68.7%. The secondary structures of tRNA genes are schematized in S1 Fig. Generally, a typical tRNA clover-leaf structure includes a 7–8 bp aminoacyl acceptor stem, a 3–5 bp TψC stem, a 5 bp anticodon stem and a 4 bp DHU stem. In the present study, most of the tRNA genes had the

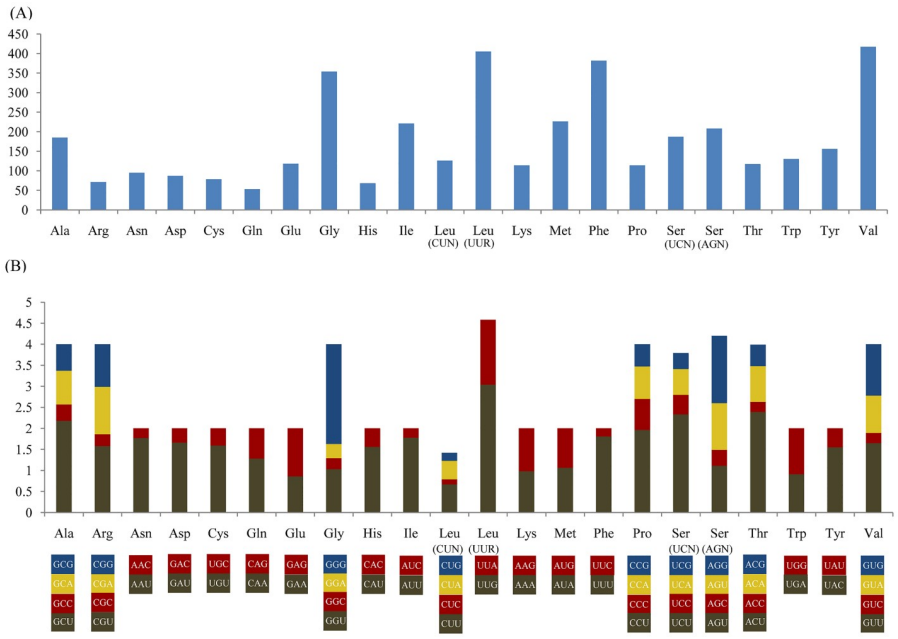

Fig 2. Codon usage (A) and the relative synonymous codon usage (RSCU) (B) of the *C. marissinica* mitogenome. Numbers to the left refer to the total number of codons (A) and the RSCU values (B). Codon families are provided on the X axis.

https://doi.org/10.1371/journal.pone.0217952.g002

typical secondary structure, except for $tRNA^{His}$, $tRNA^{Thr}$, $tRNA^{Tyr}$, $tRNA^{Ser(UCA)}$ and $tRNA^{Ser(AGA)}$. In $tRNA^{His}$, $tRNA^{Thr}$ and $tRNA^{Tyr}$, the TψC loops are incomplete, which is not observed in other vesicomyid bivalves [34–36], and this feature might be a specific character in the *C. marissinica* mitogenome. In $tRNA^{Ser(UCA)}$ and $tRNA^{Ser(AGA)}$, the DHU stems are reduced to a simple loop, as in many other bivalve mitogenomes [34,67]. Many studies have shown that the incomplete clover-leaf secondary structure of tRNA genes is common in metazoan mitogenomes and that aberrant tRNA genes can still function normally through posttranscriptional RNA editing and/or coevolved interacting factors [68–70]. Additionally, several mismatch pairs were detected within amino acid acceptors and anticodon stems in tRNA genes of *C. marissinica*. Such mismatches seem to be ubiquitous phenomena in the mitogenomes of many organisms and can also be corrected by posttranscriptional RNA editing [58,66,71–72].

Noncoding regions and gene arrangement

A total of 23 noncoding regions (totaling 2,216 bp) are distributed in the *C. marissinica* mitogenome. The longest noncoding region (1,676 bp), located between $tRNA^{Trp}$ and *nad6*, corresponds to the control region identified in most other vesicomyids. The nucleotide content of the 1,676 bp control region is 34.25% A, 39.02% T, 16.29% G, and 10.44% C. The A + T content (73.27%) of this region is higher than that of other regions in the *C. marissinica* mitogenome (Table 2). In general, the mitochondrial control region is subjected to less evolutionary pressure than PCGs and thus has the highest variation in the whole mitogenome [73–74].

Additionally, in the mitochondrial control region of *C. marissinica*, we found a tandemly arranged repeated sequence, which was 354 bp in length (positions 12,675–13,028), including three identical tandem repeat units of 118 bp (Fig 3). The tandem repeat sequence could be folded into stem-loop secondary structures with minimized free energy (Fig 3), which is a common phenomenon in invertebrates [16,63,66,75]. The control region in the mitogenome

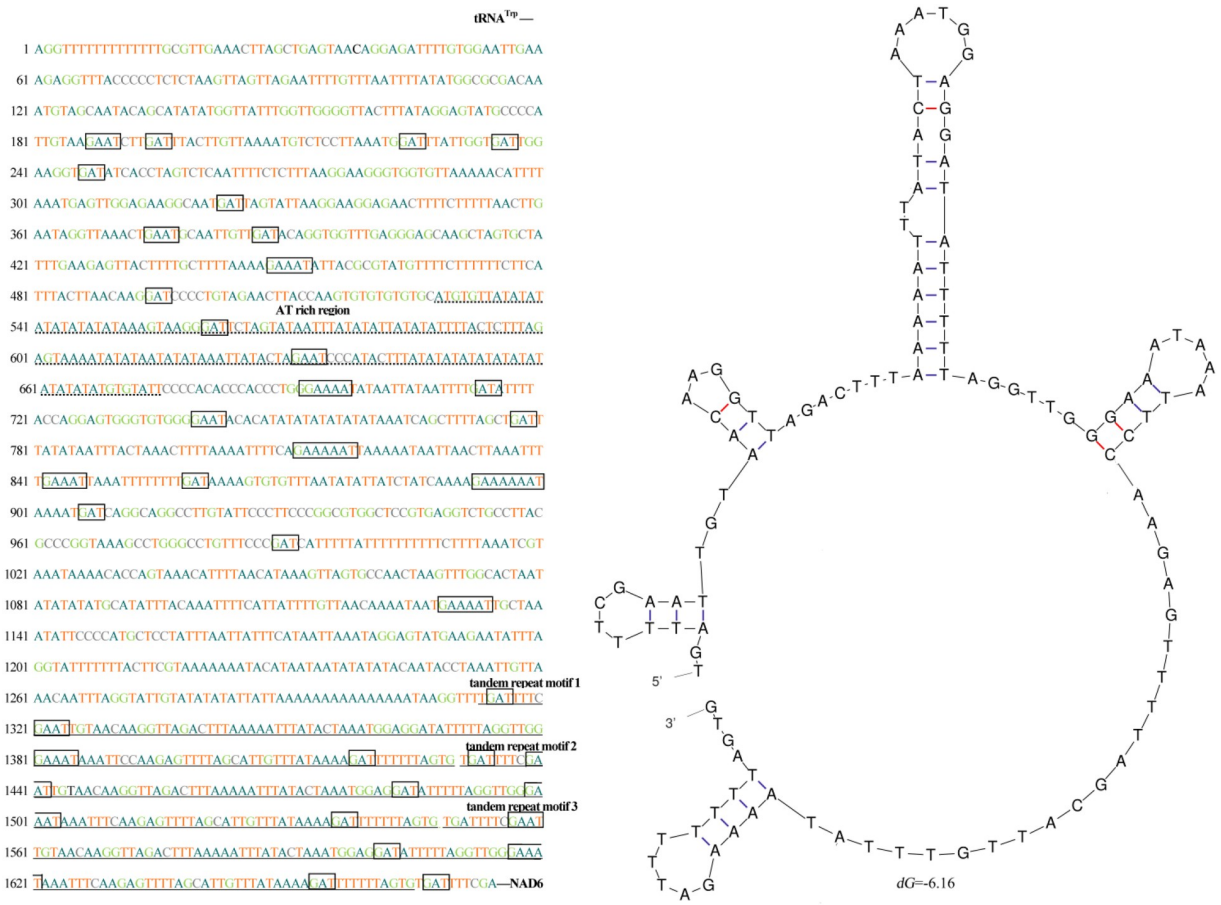

Fig 3. Nucleotide sequences and stem-loop structures of the tandem repeat motifs in the control region (CR) of the *C. marissinica* mitogenome. The CR is flanked by sequences encoding *tRNA*^{Trp} and *nad6*. The CR consists of certain patterns, such as special G(A)$_n$T motifs (marked with a box), AT-rich regions and tandem repeat motifs.

https://doi.org/10.1371/journal.pone.0217952.g003

is essential for transcription and replication in animals [76–77]. Therefore, the stem-loop structures mentioned above may play an important role in gene replication and regulation. In addition, some other peculiar patterns, such as special "G(A)$_n$T" motifs and AT-rich sequences, were observed in the control region of the *C. marissinica* mitogenome (Fig 3). Furthermore, similar characteristics (e.g., repetitive elements, G(A)$_n$T motifs and AT-rich sequences) were also observed in the deep-sea anemone *Bolocera* sp., alvinocaridid shrimp *Shinkaicaris leurokolos* and spongicolid shrimp *Spongiocaris panglao* [16,63,66]. In view of the particularity of the deep-sea chemosynthetic environment, we speculate that these special control region elements are involved in the regulation of replication and transcription of the mitogenome and may play some role in helping organisms adapt to extreme deep-sea habitats.

In contrast to other metazoans, the Mollusca showed frequent and extensive variation in gene arrangement, and among them, bivalves showed more gene order variation in their mitogenomes [78–80]. Here, a comparison of the *C. marissinica* mitogenome with the other twelve Heterodonta mitogenomes is shown in Fig 4. All thirteen Heterodonta mitogenomes come from two orders (five families): Myoida (family Hiatellidae) and Veneroida (family Tellinidae, family Mactridae, family Veneridae and family Vesicomyidae). Among the Heterodonta mitogenomes analyzed in the present study, the gene arrangement has a distinct difference between

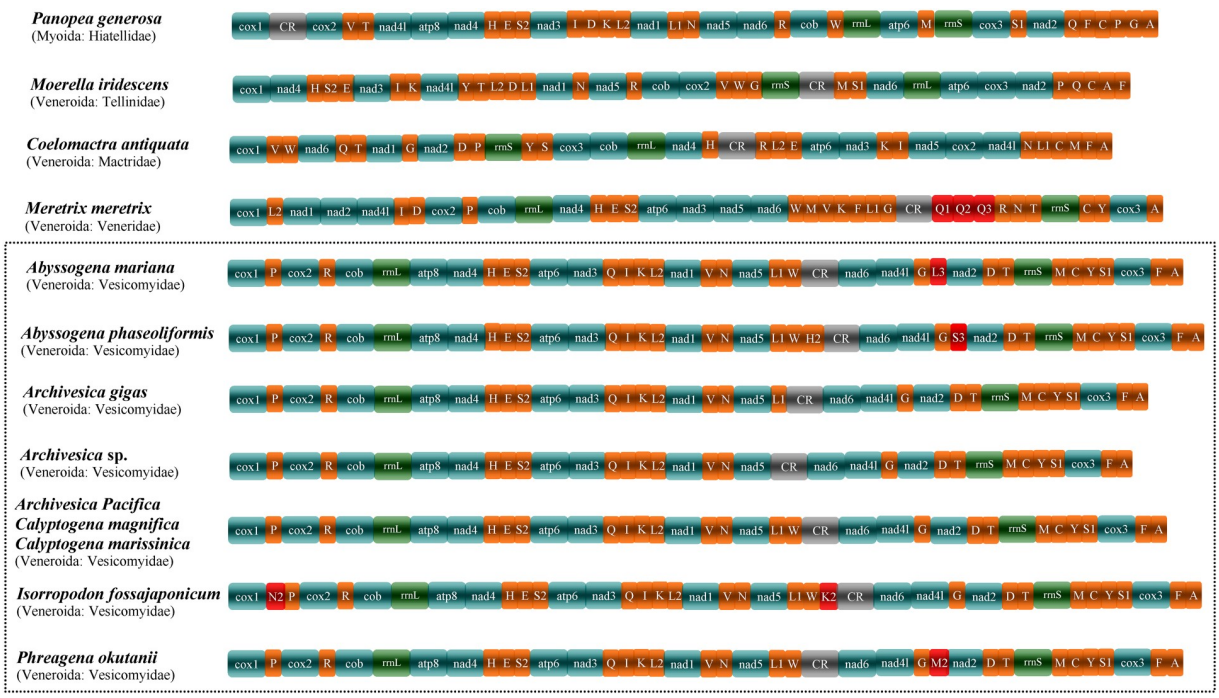

Fig 4. Mitochondrial gene arrangement of 13 species in the subclass Heterodonta (*Panopea generosa*, *Moerella iridescens*, *Coelomactra antiquata*, *Meretrix meretrix* and 9 vesicomyid bivalves). CR indicates the control region. Genes for tRNAs are displayed by a single letter for the corresponding amino acid, with two leucine tRNAs and two serine tRNAs differentiated by numerals. Uniquely derived gene positions of individual species are depicted in red. Sequence segments are not drawn to scale.

https://doi.org/10.1371/journal.pone.0217952.g004

the family Vesicomyidae and other species (Fig 4). In the family Vesicomyidae, we found that if the tRNA genes are not considered, the nine vesicomyid bivalves have a completely identical gene arrangement of PCGs. When compared to the "standard" mitogenome of *Ar. pacifica*, *C. magnifica* and *C. marissinica*, several additional tRNA genes were identified in *Ab. mariana* ($tRNA^{Leu3}$), *Ab. phaseoliformis* ($tRNA^{His2}$ and $tRNA^{Ser3}$), *I. fossajaponicum* ($tRNA^{Asn2}$ and $tRNA^{Lys2}$) and *Ph. okutanii* ($tRNA^{Met2}$) (Fig 4). As a general rule, additional gene copies usually obtained by gene replication and different gene copies would share some sequence identity with each other. However, analysis showed that the aforementioned additional tRNA genes have low similarity to other tRNA genes that encode the same tRNAs [34]. The remolding of tRNA genes, DNA shuffling and the point mutations in the anticodons may all provide chances for tRNA gene rearrangement within mitogenomes [3,81–82]. Furthermore, gene rearrangements usually occurred around the control regions, which are considered the replication origins. Perhaps gene replication events occur frequently in this region, and consequently, more novel gene arrangements will be found in this region. To date, there are four known mechanisms of gene rearrangements in mitogenomes: inversion, transposition, reverse transposition and tandem duplication-random losses (TDRLs) [83–84]. However, the specific mechanism of significant differences in mitochondrial gene arrangements in mollusks has not been completely clarified. With the determination of mitogenomes in more species of this phylum, the mechanism of large-scale rearrangement of mitochondrial genes in mollusks will be identified by further comparing and summarizing the rules of gene arrangement among different species.

Phylogenetic relationships

Since several vesicomyid bivalves have incomplete mitogenomes at present, phylogenetic analyses were performed based on nucleotide and amino acid sequences of 9 mitochondrial PCGs (*atp6*, *cox1*, *cox2*, *cox3*, *cob*, *nad1*, *nad3*, *nad4*, and *nad5*) and 2 rRNA genes by maximum likelihood (ML) and Bayesian inference (BI) methods (Fig 5, S2–S4 Figs). The tree topologies resulting from the BI and ML analyses were not the same. There are two potential reasons for this discrepancy: one is that the presence of noncoding rRNA genes made the databases of nucleotides and amino acids different, and the other is the fact that several clades are represented by only one or two species each. The phylogenetic analyses clustered *C. marissinica* with the previously reported vesicomyid bivalves with high support values (Fig 5). In all phylogenetic trees, the family Vesicomyidae first clustered well with Veneridae and then united with Mactridae, which corroborates earlier studies of phylogenetic relationships based on the concatenated 12 PCGs and 2 rRNA genes [34–36]. *Calyptogena* (*sensu lato*) is the most diverse group of deep-sea vesicomyid bivalves in the western Pacific region and its marginal seas. Until now, the composition, evolutionary position and level of the genus *Calyptogena* have been the subject of discussion [85–87]. Phylogenetic reconstruction using the cytochrome oxidase *c* subunit I (*cox1*) gene showed that *C. marissinica* was clearly nested within a fully supported monophyletic clade corresponding to *Calyptogena sensu lato* and consisting of all included *Calyptogena* (*sensu lato*) species [32]. Notably, in our studies, *C. marissinica* showed a close genetic relationship with the *Akebiconcha* species (Fig 5). Therefore, additional mitogenomes of a greater number of vesicomyid bivalves, combined with morphological characters, are necessary to determine the phylogenetic relationships among members of this family.

Positive selection analysis

Purifying selection is the predominant force in the evolution of mitogenomes, but because mitochondria are the main sites of aerobic respiration and are essential for energy metabolism, weak and/or episodic positive selection may occur against this background of strong purifying selection under reduced oxygen availability or greater energy requirements [88–89]. As proven by many studies, mitochondrial PCGs underwent positive selection in animals that survived in hypoxic environments or had higher energy demands for locomotion, such as Tibetan humans, Ordovician bivalves, diving cetaceans and flying insects [19, 90–92].

Considering that the deep-sea chemosynthetic ecosystemsmay impact the function of mitochondrial genes, we examined potential positive selection in the Vesicomyidae lineage using CodeML from the PAML package. Although different tree-building methods were used, the results of positive selection analyses were generally consistent (Table 3). In the analysis of branch models, the ω (*dN*/*dS*) ratio calculated under the one-ratio model (M_0) was 0.02272 for the 13 mitochondrial PCGs of sampled Heterodonta bivalves, suggesting that these genes have experienced constrained selection pressure to maintain function. Then, in the comparison of the one-ratio model (M_0) and the free-ratio model (M_1), the LRTs indicated that the free-ratio model fit the data better than the one-ratio model (Table 3), which means that the ω ratios are indeed different among lineages. Furthermore, the two-ratio model (M_2) was also found to fit the data better than the one-ratio model (Table 3) when the family Vesicomyidae was set as a foreground branch. The ω ratio of the Vesicomyidae branch was almost treble that of other branches ($\omega_1 = 0.06398$ and $\omega_0 = 0.02278$), indicating divergence in selection pressure between vesicomyid bivalves and other shallow-sea Heterodonta species. However, the ω ratio of the family Vesicomyidae ($\omega_1 = 0.06398$) was still significantly less than 1. This result is consistent with the known functional significance of mitochondria as a respiration chain necessary for electron transport and OXPHOS [93].

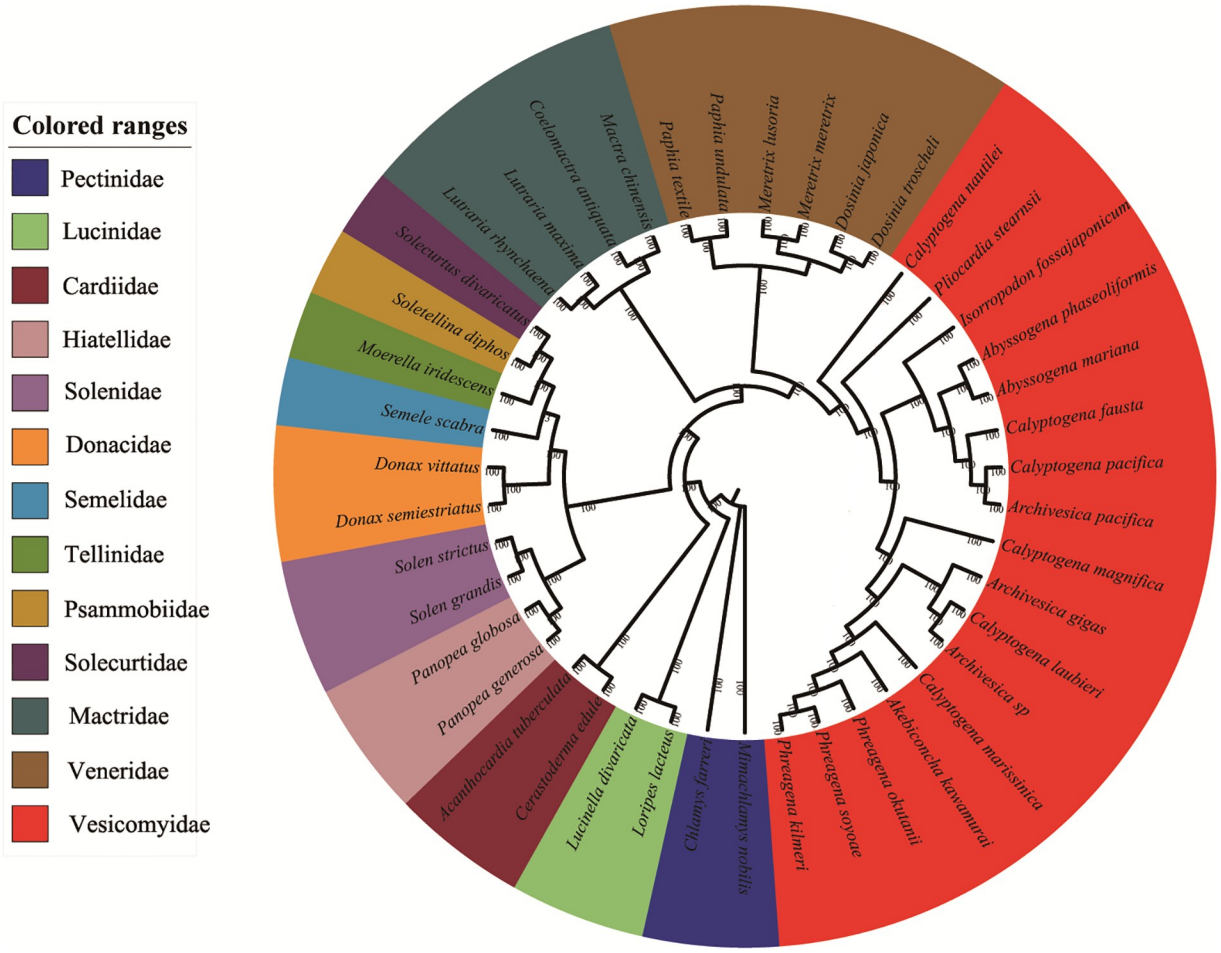

Fig 5. Phylogenetic tree derived from Bayesian analyses based on concatenated nucleotide sequences of 9 mitochondrial PCGs (*cox1*, *cox2*, *cox3*, *cob*, *atp6*, *nad1*, *nad4*, *nad5*, and *nad6*) and 2 ribosomal RNA genes (*rrnS* and *rrnL*). Numbers on branches are Bayesian posterior probabilities (percent). Two Pectinidae species belonging to the subclass Pteriomorphia were used as outgroups.

https://doi.org/10.1371/journal.pone.0217952.g005

Moreover, many studies have shown that positive selection often occurs over a short period of evolutionary time and acts on only a few sites; thus, the signal for positive selection is usually swamped by those for continuous purifying selection that occur on most sites in a gene sequence [88,94]. In the present study, branch-site models were used to detect possible positively selected sites in the vesicomyid bivalves (Table 4). Ten residues, which were located in *cox1*, *cox3*, *cob*, *nad2*, *nad4* and *nad5*, were identified as positively selected sites with high BEB values (> 95%).

It is well known that mitochondrial PCGs play a key role in the oxidative phosphorylation pathway; the above ten amino acid mutation sites are components of the respiratory chain and therefore may have important functions. As the first and the largest enzyme complex in the respiratory chain, the NADH dehydrogenase complex exercises the functions of proton pumps, and variation in loci may interfere with the efficiency of the proton-pumping process, which then affect metabolic performance [91]. In this work, there were four positively selected sites located in the *nad2*, *nad4* and *nad5* genes (subunits 2, 4 and 5 of NADH deshydrogenase). Under the deep-sea chemosynthetic enviroment, survival may require a modified and adapted energy metabolism, and evidences of adaptive evolution in the NADH dehydrogenase complex

Table 3. CODEML analyses of selection pressure on mitochondrial genes in the Vesicomyidae lineage.

Trees	Models	lnL	Parameter estimates	Models compared	2ΔL	*p*-value
Branch models						
Bayesian tree	M0	-203672.1001	$\omega = 0.02272$			
	Two-ratio	-203666.6298	$\omega_0 = 0.02278$ $\omega_1 = 0.06398$	Two-ratio vs. M0	10.94072	0.00094
	Free-ratio	-202667.8186		Free-ratio vs. M0	2008.56299	0.00000
ML tree	M0	-203672.1001	$\omega = 0.02272$			
	Two-ratio	-203666.6298	$\omega_0 = 0.02278$ $\omega_1 = 0.06398$	Two-ratio vs. M0	10.94072	0.00094
	Free-ratio	-202747.0065		Free-ratio vs. M0	1850.18729	0.00000
Branch-site models						
Bayesian tree	Null model	-202664.0952	$P_0 = 0.77667$ $P_1 = 0.02562$ $P_{2a} = 0.19139$ $P_{2b} = 0.00631$			
			$\omega_0 = 0.02110$ $\omega_1 = 1.00000$ $\omega_{2a} = 1.00000$ $\omega_{2b} = 1.00000$			
	Model A	-202663.7531	$P_0 = 0.78464$ $P_1 = 0.02590$ $P_{2a} = 0.18340$ $P_{2b} = 0.00605$	Model A vs. Null model	0.68422	0.40814
			$\omega_0 = 0.02115$ $\omega_1 = 1.00000$ $\omega_{2a} = 1.21998$ $\omega_{2b} = 1.21998$			
ML tree	Null model	-202664.0952	$P_0 = 0.77667$ $P_1 = 0.02562$ $P_{2a} = 0.19140$ $P_{2b} = 0.00631$			
			$\omega_0 = 0.02110$ $\omega_1 = 1.00000$ $\omega_{2a} = 1.00000$ $\omega_{2b} = 1.00000$			
	Model A	-202663.7531	$P_0 = 0.77667$ $P_1 = 0.02562$ $P_{2a} = 0.19139$ $P_{2b} = 0.00631$	Model A vs. Null model	0.68422	0.40814
			$\omega_0 = 0.02115$ $\omega_1 = 1.00000$ $\omega_{2a} = 1.22003$ $\omega_{2b} = 1.22003$			

https://doi.org/10.1371/journal.pone.0217952.t003

have been reported in mitogenome of Tibetan horses, Chinese snub-nosed monkeys and Tibetan loaches [20,22,25]. Two residues in the *cob* gene were identified to be under positive selection. As a relatively conserved gene, *cob* plays a fundamental role in energy production in mitochondria. It catalyzes reversible electron transfer from ubiquinol to cytochrome *c* coupled to proton translocation [95]. Wide variation in the properties of amino acids was observed in functionally important regions of *cob* in species with more specialized metabolic requirements, such as adaptation to a low-energy diet or large body size and adaptation to unusual oxygen requirements or low-temperature environments [91,96]. Cytochrome *c* oxidase, which catalyzes the terminal reduction of oxygen and whose catalytic core is encoded by three mitochondrial protein-coding genes (*cox1*, *cox2* and *cox3*), has been proven to be a particularly important target of positive selection during hypoxia adaptation [97–98]. Studies have shown that when cells of the organisms are exposed to anoxia, the cytochrome *c* oxidase are required for the produced reactive oxygen species (ROS), and the increase in ROS concentration serves to stabilize Hif-1α, which then leads to the induction of Hif-1-dependent nuclear hypoxic

Table 4. Possible sites under positive selection in the Vesicomyidae lineage.

Bayesian tree				ML tree			
Gene	Codon	Amino acid	BEB values	Gene	Codon	Amino acid	BEB values
cox1	529	W	0.967	*cox1*	529	W	0.967
cox3	998	G	0.956	*cox3*	998	G	0.956
	1018	W	0.962		1018	W	0.962
	1021	T	0.954		1021	T	0.954
cob	1131	K	0.982	*cob*	1131	K	0.982
	1432	A	0.959		1432	A	0.959
nad2	2043	K	0.960	*nad2*	2043	K	0.960
nad4	2388	E	0.951	*nad4*	2388	E	0.951
nad5	2734	P	0.975	*nad5*	2734	P	0.975
	2773	S	0.951		2773	S	0.951

https://doi.org/10.1371/journal.pone.0217952.t004

genes [99–100]. Four positively selected residues were detected in the *cox1* and *cox3* genes. For *C. marissinica*, functional modification mediated by positively selected mutations may increase the affinity between the enzyme and oxygen, thus allowing the efficient utilization of oxygen under hypoxia and maintaining essential metabolic levels.

The environment of deep-sea hydrothermal vents and cold seeps is characterized by darkness, a lack of photosynthesis-derived nutrients, high hydrostatic pressure, variable temperatures, low dissolved oxygen, and high concentrations of hydrogen sulfide (H_2S), methane (CH_4) and heavy metals, such as iron, copper and zinc [9, 101]. Previous studies have confirmed that all of the above environmental factors influence the process of mitochondrial aerobic respiration; for example, thirty potentially important adaptive residues were identified in the mitogenome of *S. leurokolos* and revealed the mitochondrial genetic basis of hydrothermal vent adaptation in alvinocaridid shrimp [16]. Similar findings have been reported in other deep-sea macrobenthos, such as the sea anemone *Bolocera* sp., starfish *Freyastera benthophila* and sea cucumber *Benthodytes marianensis* [66,102–103]. In the present study, ten potentially adaptive residues were identified in the *cox1*, *cox3*, *cob*, *nad2*, *nad4* and *nad5* genes, supporting the adaptive evolution of the mitogenome of *C. marissinica*. Our results establishes a necessary foundation to understand how the deep-sea vesicomyid bivalves maintain aerobic respiration for sufficient energy in harsh deep-sea chemosynthetic environment at the mitochondrial level.

Conclusion

This study characterized the complete mitogenome of the deep-sea vesicomyid bivalve *C. marissinica*, which is 17,374 bp in length and encodes 37 typical mitochondrial genes, including 13 PCGs, 2 rRNA genes, and 22 tRNA genes. All of these genes are encoded on the heavy strand. We analyzed the mitogenome organization, codon usage, control region features, gene arrangement, phylogenetic relationships and positive selection of *C. marissinica*. In the mitogenome of *C. marissinica*, tandem repeat sequences, "$G(A)_nT$" motifs and AT-rich sequences were detected. In the family Vesicomyidae, we found that if the tRNA genes are not considered, the sequenced vesicomyid bivalves have a completely identical arrangement of PCGs. The phylogenetic analyses clustered *C. marissinica* with previously reported vesicomyid bivalves with high support values. Ten residues located in *cox1*, *cox3*, *cob*, *nad2*, *nad4* and *nad5* were inferred to be positively selected sites along the branches leading to vesicomyid bivalves, which may indicate that the genes were under positive selection pressure. The findings of this study could help deepen our understanding of the molecular mechanisms of adaptive evolution at the mitochondrial level in deep-sea organisms.

Supporting information

S1 Table. Species used for phylogenetic reconstructions.
(DOCX)

S2 Table. Species used for CodeML analyses of selective pressure on mitochondrial genes.
(DOCX)

S1 Fig. Putative secondary structures for the 22 transfer RNAs of the *C. marissinica* mitogenome.
(TIF)

S2 Fig. Phylogenetic trees derived from ML analyses based on nucleotide sequences of 9 mitochondrial protein-coding genes and 2 ribosomal RNA genes.
(TIF)

S3 Fig. Phylogenetic trees derived from Bayesian analyses based on amino acid sequences of 9 mitochondrial protein-coding genes.
(TIF)

S4 Fig. Phylogenetic trees derived from ML analyses based on amino acid sequences of 9 mitochondrial protein-coding genes.
(TIF)

Acknowledgments

The authors thank the captains and crews of the R/V Tan Suo Yi Hao and the pilots of the HOV "Shen Hai Yong Shi" for technical support.

Author Contributions

Conceptualization: Mei Yang, Xinzheng Li.

Data curation: Mei Yang, Xinzheng Li.

Formal analysis: Mei Yang.

Funding acquisition: Mei Yang, Lin Gong, Xinzheng Li.

Investigation: Mei Yang, Lin Gong, Jixing Sui, Xinzheng Li.

Methodology: Mei Yang.

Project administration: Xinzheng Li.

Resources: Mei Yang, Xinzheng Li.

Software: Mei Yang.

Supervision: Mei Yang, Xinzheng Li.

Validation: Mei Yang, Jixing Sui, Xinzheng Li.

Visualization: Mei Yang, Xinzheng Li.

Writing – original draft: Mei Yang, Xinzheng Li.

Writing – review & editing: Mei Yang, Xinzheng Li.

References

1. Martijn J, Vosseberg J, Guy L, Offre P, Ettema TJG. Deep mitochondrial origin outside the sampled alphaproteobacteria. Nature. 2018; 557: 101–105. https://doi.org/10.1038/s41586-018-0059-5 PMID: 29695865
2. Wolstenholme DR. Animal mitochondrial DNA: Structure and evolution. International Review of Cytology. 1992; 141: 173–216. PMID: 1452431
3. Boore JL. Animal mitochondrial genomes. Nucleic Acids Research. 1999; 27: 1767–1780. https://doi.org/10.1093/nar/27.8.1767 PMID: 10101183
4. Hebert P, Cywinska A, Ball S, Waard J. Biological identification through DNA barcodes. Proceedings of the Royal Society B Biological Sciences. 2002; 270: 313–321. https://doi.org/10.1098/rspb.2002.2218 PMID: 12614582
5. Gissi C, Iannelli F, Pesole G. Evolution of the mitochondrial genome of Metazoa as exemplified by comparison of congeneric species. Heredity. 2008; 101: 301–320. http://doi.org/10.1038/hdy.2008.62 PMID: 18612321
6. Tan MH, Gan HM, Lee YP, Linton S, Grandjean F, Bartholomei-Santos ML, et al. ORDER within the chaos: Insights into phylogenetic relationships within the Anomura (Crustacea: Decapoda) from mitochondrial sequences and gene order rearrangements. Molecular Phylogenetics and Evolution. 2018; 127: 320–331. https://doi.org/10.1016/j.ympev.2018.05.015 PMID: 29800651

7. Schuster A, Vargas S, Knapp IS, Pomponi SA, Toonen RJ, Erpenbeck D, et al. Divergence times in demosponges (Porifera): first insights from new mitogenomes and the inclusion of fossils in a birth-death clock model. BMC Evolutionary Biology. 2018; 18: 114. https://dx.doi.org/10.1186/s12862-018-1230-1 PMID: 30021516
8. Sibuet M, Olu K. Biogeography, biodiversity and fluid dependence of deep-sea cold-seep communities at active and passive margins. Deep-Sea Research II: Topical Studies in Oceanography. 1998; 45: 517–567.
9. Van Dover CL, German CR, Speer KG, Parson LM, Vrijenhoek RC. Evolution and Biogeography of Deep-Sea Vent and Seep Invertebrates. Science. 2002; 295: 1253–1257. https://doi.org/10.1126/science.1067361 PMID: 11847331
10. Martin W, Baross J, Kelley D, Russell MJ. Hydrothermal vents and the origin of life. Nature Review Microbiology. 2008; 6: 805–814. https://doi.org/10.1038/nrmicro1991 PMID: 18820700
11. Vrijenhoek RC. Genetic diversity and connectivity of deep-sea hydrothermal vent metapopulations. Molecular Ecology. 2010; 19: 4391–4411. https://doi.org/10.1111/j.1365-294X.2010.04789.x PMID: 20735735
12. Sun J, Zhang Y, Xu T, Zhang Y, Mu H, Zhang Y, et al. Adaptation to deep-sea chemosynthetic environments as revealed by mussel genomes. Nature Ecology Evolution. 2017; 1: 121. https://doi.org/10.1038/s41559-017-0121 PMID: 28812709
13. Zheng P, Wang MX, Li CL, Sun XQ, Wang XC, Sun Y, et al. Insights into deep-sea adaptations and host-symbiont interactions: A comparative transcriptome study on *Bathymodiolus* mussels and their coastal relatives. Molecular Ecology. 2017; 26: 5133–5148. https://doi.org/10.1111/mec.14160 PMID: 28437568
14. Hui M, Cheng J, Sha ZL. First comprehensive analysis of lysine acetylation in *Alvinocaris longirostris* from the deep-sea hydrothermal vents. BMC Genomics. 2018; 19: 352. https://doi.org/10.1186/s12864-018-4745-3 PMID: 29747590
15. Lan Y, Sun J, Xu T, Chen C, Tian RM, Qiu JW, et al. *De novo* transcriptome assembly and positive selection analysis of an individual deep-sea fish. BMC Genomics. 2018; 19: 394. https://doi.org/10.1186/s12864-018-4720-z PMID: 29793428
16. Sun SE, Hui M, Wang MX, Sha ZL. The complete mitochondrial genome of the alvinocaridid shrimp *Shinkaicaris leurokolos* (Decapoda, Caridea): Insight into the mitochondrial genetic basis of deep-sea hydrothermal vent adaptation in the shrimp. Comparative Biochemistry and Physiology-Part D. 2018; 25: 42–52. https://doi.org/10.1016/j.cbd.2017.11.002 PMID: 29145028
17. Wang ZF, Shi XJ, Sun LX, Bai YZ, Zhang DZ, Tang BP. Evolution of mitochondrial energy metabolism genes associated with hydrothermal vent adaption of Alvinocaridid shrimps. Genes Genomics. 2017; 39: 1367–1376. https://doi.org/10.1007/s13258-017-0600-1
18. Plazzi F, Puccio G, Passamonti M. Burrowers from the Past: Mitochondrial Signatures of Ordovician Bivalve Infaunalization. Genome Biology and Evolution. 2017; 9: 956–967. https://doi.org/10.1093/gbe/evx051 PMID: 28338965
19. Gu ML, Dong XQ, Shi L, Shi L, Lin KQ, Huang XQ, et al. Differences in mtDNA whole sequence between Tibetan and Han populations suggesting adaptive selection to high altitude. Gene. 2012; 496: 37–44. https://doi.org/10.1016/j.gene.2011.12.016 PMID: 22233893
20. Yu L, Wang XP, Ting N, Zhang YP. Mitogenomic analysis of Chinese snub-nosed monkeys: Evidence of positive selection in NADH dehydrogenase genes in high-altitude adaptation. Mitochondrion. 2011; 11: 497–503. https://doi.org/10.1016/j.mito.2011.01.004 PMID: 21292038
21. Xu SQ, Yang YZ, Zhou J, Jin GE, Chen YT, Wang J, et al. A mitochondrial genome sequence of the Tibetan antelope (*Pantholops hodgsonii*). Genomics, proteomics & bioinformatics. 2005; 3: 5–17. https://doi.org/10.1016/S1672-0229(05)03003-2 PMID: 16144518
22. Ning T, Xiao H, Li J, Hua S, Zhang YP. Adaptive evolution of the mitochondrial ND6 gene in the domestic horse. Genetics and Molecular Research. 2010; 9: 144–150. https://doi.org/10.4238/vol9-1gmr705 PMID: 20198570
23. Wang ZF, Yonezawa T, Liu B, Ma T, Shen X, Su JP, et al. Domestication relaxed selective constraints on the yak mitochondrial genome. Molecular Biology and Evolution. 2011; 28:1553–1556. https://doi.org/10.1093/molbev/msq336 PMID: 21156878
24. Zhou TC, Shen XJ, Irwin DM, Shen YY, Zhang YP. Mitogenomic analyses propose positive selection in mitochondrial genes for high-altitude adaptation in galliform birds. Mitochondrion. 2014; 18: 70–75. https://doi.org/10.1016/j.mito.2014.07.012 PMID: 25110061
25. Wang Y, Shen YJ, Feng CG, Zhao K, Song ZB, Zhang YP, et al. Mitogenomic perspectives on the origin of Tibetan loaches and their adaptation to high altitude. Scientific Reports. 2016; 6: 29690. https://doi.org/10.1038/srep29690 PMID: 27417983

26. Boss KJ, Turner RD. The giant white clam from the Galapagos Rift, *Calyptogena magnifica* species novum. Malacologia. 1980; 20: 161–194.
27. Bennett BA, Smith CR, Glaser B, Maybaum HL. Faunal community structure of achemoautortophic assemblage on whale bones in the deep northeast Pacific Ocean. Marine Ecology Progress. 1994; 108: 205–223.
28. Cosel RV, Salas C, Høisæter T. Vesicomyidae (Mollusca: Bivalvia) of the genera *Vesicomya*, *Waisiuconcha*, *Isorropodon* and *Callogonia* in the eastern Atlantic and the Mediterranean. Sarsia, 86(4–5): 333–366. https://doi.org/10.1080/00364827.2001.10425523.
29. Krylova EM, Sahling H. Vesicomyidae (bivalvia): Current taxonomy and distribution. PLoS One. 2010; 5: e9957. https://doi.org/10.1371/journal.pone.0009957 PMID: 20376362
30. Fisher CR. Chemoautotrophic and methanotrophic symbioses in marine invertebrates. Reviews in Aquatic Sciences. 1990; 2: 399–436.
31. Krylova EM, Drozdov AL, Mironov AN. Presence of bacteria in gills of hadal bivalve "*Vesicomya*" *sergeevi* Filatova, 1971. Ruthenica. 2000; 10: 76–79.
32. Chen C, Okutani T, Liang QY, Qiu JW. A Noteworthy New Species of the Family Vesicomyidae from the South China Sea (Bivalvia: Glossoidea). Venus. 2018; 76: 29–37.
33. Liu HL, Cai SY, Zhang HB, Vrijenhoek RC. Complete mitochondrial genome of hydrothermal vent clam *Calyptogena magnifica*. Mitochondrial DNA Part A DNA Mapping, Sequencing, and Analysis. 2015; 27: 4333–4335. https://doi.org/10.3109/19401736.2015.1089488 PMID: 26462964
34. Liu HL, Cai SY, Liu J, Zhang HB. Comparative mitochondrial genomic analyses of three chemosynthetic vesicomyid clams from deep-sea habitats. Ecology and Evolution. 2018; 8: 7261–7272. https://doi.org/10.1002/ece3.4153 PMID: 30151147
35. Ozawa G, Shimamura S, Takaki Y, Takishita K, Ikuta T, Barry JP, et al. Ancient occasional host switching of maternally transmitted bacterial symbionts of chemosynthetic vesicomyid clams. Genome Biology and Evolution. 2017; 9: 2226–2236. https://doi.org/10.1093/gbe/evx166 PMID: 28922872
36. Ozawa G, Shimamura S, Takaki Y, Yokobori SI, Ohara Y, Takishita K, et al. Updated mitochondrial phylogeny of Pteriomorph and Heterodont Bivalvia, including deep-sea chemosymbiotic *Bathymodiolus* mussels, vesicomyid clams and the thyasirid clam *Conchocele cf. bisecta*. Marine Genomics. 2017; 31: 43–52. https://doi.org/10.1016/j.margen.2016.09.003 PMID: 27720682
37. Haas BJ, Salzberg SL, Zhu W, Pertea M, Allen JE, Orvis J et al. Automated eukaryotic gene structure annotation using EVidenceModeler and the Program to Assemble Spliced Alignments. Genome Biology. 2008; 9: R7. https://doi.org/10.1186/gb-2008-9-1-r7 PMID: 18190707
38. Lagesen K, Hallin P, Rødland EA, Stærfeldt HH, Rognes T, Ussery DW. RNAmmer: consistent and rapid annotation of ribosomal RNA genes. Nucleic Acids Research. 2007; 35: 3100–3108. https://doi.org/10.1093/nar/gkm160 PMID: 17452365
39. Lowe TM, Eddy SR. tRNAscan-SE: a program for improved detection of transfer RNA genes in genomic sequence. Nucleic Acids Research. 1997; 25: 955–964. https://doi.org/10.1093/nar/25.5.0955 PMID: 9023104
40. Lohse M, Drechsel O, Bock R. OrganellarGenomeDRAW (OGDRAW): a tool for the easy generation of high-quality custom graphical maps of plastid and mitochondrial genomes. Current Genetics. 2007; 52: 267–274. https://doi.org/10.1007/s00294-007-0161-y PMID: 17957369
41. Librado P, Rozas J. DnaSP v5: A software for comprehensive analysis of DNA polymorphism data. Bioinformatics. 2009; 25: 1451–1452. https://doi.org/10.1093/bioinformatics/btp187 PMID: 19346325
42. Perna NT, Kocher TD. Patterns of nucleotide composition at fourfold degenerate sites of animal mitochondrial genomes. Journal of Molecular Evolution. 1995; 41: 353–358. https://doi.org/10.1007/bf00186547 PMID: 7563121
43. Benson G. Tandem repeats finder: a program to analyze DNA sequences. Nucleic Acids Research. 1999; 27: 573–580. https://doi.org/10.1093/nar/27.2.573 PMID: 9862982
44. Zuker M. Mfold web server for nucleic acid folding and hybridization prediction. Nucleic Acids Research. 2003; 31: 3406–3415. https://doi.org/10.1093/nar/gkg595 PMID: 12824337
45. Talavera G, Castresana J. Improvement of phylogenies after removing divergent and ambiguously aligned blocks from protein sequence alignments. Systematic Biology. 2007; 56: 564–577. https://doi.org/10.1080/10635150701472164 PMID: 17654362
46. Darriba D, Taboada GL, Doallo R, Posada D. jModelTest 2: more models, new heuristics and parallel computing. Nature Methods. 2012; 9: 772. https://doi.org/10.1038/nmeth.2109 PMID: 22847109
47. Darriba D, Taboada GL, Doallo R, Posada D. ProtTest 3: fast selection of best-fit models of protein evolution. Bioinformatics. 2011; 27: 1164–1165. https://doi.org/10.1093/bioinformatics/btr088 PMID: 21335321

48. Stamatakis A. RAxML version 8: a tool for phylogenetic analysis and post-analysis of large phylogenies. Bioinformatics. 2014; 30: 1312–1313. https://doi.org/10.1093/bioinformatics/btu033 PMID: 24451623

49. Ronquist F, Teslenko M, van der Mark P, Ayres DL, Darling A, Höhna S. MrBayes 3.2: efficient bayesian phylogenetic inference and model choice across a large model space. Systematic Biology. 2012; 61: 539–542. https://doi.org/10.1093/sysbio/sys029 PMID: 22357727

50. Ohta T. The nearly neutral theory of molecular evolution. Annual Review of Ecology and Systematics. 1992; 23: 263–286. https://www.jstor.org/stable/2097289

51. Yang Z. Likelihood ratio tests for detecting positive selection and application to primate lysozyme evolution. Molecular Biology and Evolution. 1998; 15: 568–573. https://doi.org/10.1093/oxfordjournals.molbev.a025957 PMID: 9580986

52. Yang Z. PAML 4: a program package for phylogenetic analysis by maximum likelihood. Molecular Biology and Evolution. 2007; 24: 1586–1591. https://doi.org/10.1093/molbev/msm088 PMID: 17483113

53. Yang Z, Nielsen R, Goldman N, Pedersen AM. Codon-substitution models for heterogeneous selection pressure at amino acid sites. Genetics. 2000; 155: 431–449. PMID: 10790415

54. Nielsen R, Yang Z. Likelihood models for detecting positively selected amino acid sites and applications to the HIV-1 envelope gene. Genetics. 1998; 148: 929–936. PMID: 9539414

55. Yang Z, Wong WS, Nielsen R. Bayes empirical bayes inference of amino acid sites under positive selection. Molecular Biology and Evolution. 2005; 22: 1107–1118. https://doi.org/10.1093/molbev/msi097 PMID: 15689528

56. Xu X, Wu X, Yu Z. The mitogenome of *Paphia euglypta* (Bivalvia: Veneridae) and comparative mitogenomic analyses of three venerids. Genome. 2010; 53: 1041–1052. https://doi.org/10.1139/G10-096 PMID: 21164537

57. Liao F, Wang L, Wu S, Li YP, Zhao L, Huang GM, et al. The complete mitochondrial genome of the fall webworm, *Hyphantria cunea* (Lepidoptera: Arctiidae). International Journal of Biological Sciences. 2010; 6: 172–186. https://doi.org/10.7150/ijbs.6.172 PMID: 20376208

58. Wang ZL, Chao L, Fang WY, Yu XP. The Complete Mitochondrial Genome of two *Tetragnatha* Spiders (Araneae: Tetragnathidae): Severe Truncation of tRNAs and Novel Gene Rearrangements in Araneae. International Journal of Biological Sciences. 2016; 12: 109–119. https://doi.org/10.7150/ijbs.12358 PMID: 26722222

59. Ojala D, Montoya J, Attardi G. tRNA punctuation model of RNA processing in human mitochondria. Nature. 1981; 290: 470–474. https://doi.org/10.1038/290470a0 PMID: 7219536

60. Dreyer H, Steiner G. The complete sequences and gene organisation of the mitochondrial genome of the heterodont bivalves *Acanthocardia tuberculata* and *Hiatella arctica*– and the first record for a putative Atp*ase subunit 8* gene in marine bivalves. Frontiers in Zoology. 2006; 3: 13. https://dx.doi.org/10.1186/1742-9994-3-13 PMID: 16948842

61. Salvato P, Simonato M, Battisti A, Negrisolo E. The complete mitochondrial genome of the bag-shelter moth *Ochrogaster lunifer* (Lepidoptera, Notodontidae). BMC Genomics. 2008; 9: 331. https://dx.doi.org/10.1186/1471-2164-9-331 PMID: 18627592

62. Yu H, Li Q. Complete mitochondrial DNA sequence of *Crassostrea nippona*: comparative and phylogenomic studies on seven commercial *Crassostrea* species. Molecular Biology Reports. 2012; 39: 999–1009. https://doi.org/10.1007/s11033-011-0825-z PMID: 21562763.

63. Sun SE, Sha ZL, Wang YR. Complete mitochondrial genome of the first deep-sea spongicolid shrimp *Spongiocaris panglao* (Decapoda: Stenopodidea): Novel gene arrangement and the phylogenetic position and origin of Stenopodidea. Gene. 2018; 676: 123–138. https://doi.org/10.1016/j.gene.2018.07.026 PMID: 30021129

64. Brown WM. The mitochondrial genome of animals. In: Molecular Evolutionary Genetics. New York: Plenum Press; 1985.

65. Chai HN, Du YZ, Zhai BP. Characterization of the complete mitochondrial genome of *Cnaphalocrocis medinalis* and *Chilo suppressalis* (Lepidoptera: Pyralidae). International Journal of Biological Sciences. 2012; 8: 561–579. https://doi.org/10.1007/s10126-005-0004-0 PMID: 22532789

66. Zhang B, Zhang YH, Wang X, Zhang HX, Lin Q. The mitochondrial genome of a sea anemone *Bolocera* sp. exhibits novel genetic structures potentially involved in adaptation to the seep-sea environment. Ecology and Evolution. 2017; 7: 4951–4962. https://doi.org/10.1002/ece3.3067 PMID: 28690821

67. Plazzi F, Ribani A, Passamonti M. The complete mitochondrial genome of *Solemya velum* (Mollusca: Bivalvia) and its relationships with conchifera. BMC Genomics. 2013; 14: 409. https://doi.org/10.1186/1471-2164-14-409 PMID: 23777315

68. Okimoto R, Macfarlane JL, Clary DO, Wolstenholme DR. The mitochondrial genomes of two nematodes, *Caenorhabditis elegans* and *Ascaris suum*. Genetics. 1992; 130: 471–498. PMID: 1551572

69. Ohtsuki T, Kawai G, Watanabe K. The minimal tRNA: unique structure of *Ascaris suum* mitochondrial tRNA(Ser)(UCU) having a short T arm and lacking the entire D arm. FEBS Letter. 2002; 514: 37–43. https://doi.org/10.1016/s0014-5793(02)02328-1 PMID: 11904178

70. Chimnaronk S, Gravers Jeppesen M, Suzuki T, Nyborg J, Watanabe K. Dualmode recognition of noncanonical tRNAs(Ser) by seryl-tRNA synthetase in mammalian mitochondria. Embo Journal. 2005; 24: 3369–3379. https://doi.org/10.1038/sj.emboj.7600811 PMID: 16163389

71. Lavrov DV, Brown WM, Boore JL. A novel type of RNA editing occurs in the mitochondrial tRNAs of the centipede *Lithobius forficatus*. Proceedings of the National Academy of Sciences of the United States of America. 2000; 97: 13738–13742. https://doi.org/10.1073/pnas.250402997 PMID: 11095730

72. Miller AD, Murphy NP, Burridge CP, Austin CM. Complete mitochondrial DNA sequences of the decapod crustaceans *Pseudocarcinus gigas* (Menippidae) and *Macrobrachium rosenbergii* (Palaemonidae). Marine Biotechnology. 2005; 7: 339–349. https://doi.org/10.1007/s10126-004-4077-y PMID: 15902543

73. Aquadro CF, Greenberg BD. Human mitochondrial DNA variation and evolution: Analysis of nucleotide sequences from seven individuals. Genetics. 1983; 103: 287–312. PMID: 6299878

74. Marshall HD, Baker AJ. Structural conservation and variation in the mitochondrial control region of fringilline finches (*Fringilla* spp.) and the greenfinch (*Carduelis chloris*). Molecular Biology and Evolution. 1997; 14: 173–184. https://doi.org/10.1093/oxfordjournals.molbev.a025750 PMID: 9029795

75. Flot JF, Tillier S. The mitogenome of *Pocillopora* (Cnidaria: Scleractinia) contains two variable regions: The putative D-loop and a novel ORF of unknown function. Gene. 2007; 401: 80–87. https://doi.org/10.1016/j.gene.2007.07.006 PMID: 17716831

76. Stanton DJ, Daehler LL, Moritz CC, Brown WM. Sequences with the potential to form stem-and-loop structures are associated with coding-region duplications in animal mitochondrial DNA. Genetics. 1994; 137: 233–241. PMID: 8056313

77. Fernández-Silva P, Enriquez JA, Montoya J. Replication and transcription of mammalian mitochondrial DNA. Experimental Physiology. 2003; 88: 41–56. PMID: 12525854

78. Serb JM, Lydeard C. Complete mtDNA sequence of the north American freshwater mussel, *Lampsilis ornata* (Unionidae): an examination of the evolution and phylogenetic utility of mitochondrial genome organization in Bivalvia (Mollusca). Molecular Biology and Evolution. 2003; 20: 1854–1866. https://doi.org/10.1093/molbev/msg218 PMID: 12949150

79. Ren J, Shen X, Jiang F, Liu B. The mitochondrial genomes of two scallops, *Argopecten irradians* and *Chlamys farreri* (Mollusca: Bivalvia): the most highly rearranged gene order in the family Pectinidae. Journal of Molecular Evolution. 2009; 70: 57–68. https://doi.org/10.1007/s00239-009-9308-4 PMID: 20013337

80. Milbury CA, Gaffney PM. Complete mitochondrial DNA sequence of the eastern oyster *Crassostrea virginica*. Marine Biotechnology. 2005; 7: 697–712. https://doi.org/10.1007/s10126-005-0004-0 PMID: 16132463

81. Kumazawa Y, Miura S, Yamada C, Hashiguchi Y. Gene rearrangements in gekkonid mitochondrial genomes with shuffling, loss, and reassignment of tRNA genes. BMC Genomics. 2014; 15: 930. https://doi.org/10.1186/1471-2164-15-930 PMID: 25344428

82. Sahyoun AH, Hölzer M, Jühling F, Hölzer zu Siederdissen C, Al-Arab M, Tout K, et al. Towards a comprehensive picture of alloacceptor tRNA remolding in metazoan mitochondrial genomes. Nucleic Acids Research. 2015; 43: 8044–8056. https://doi.org/10.1093/nar/gkv746 PMID: 26227972

83. Boore JL, Brown WM. Big trees from little genomes: mitochondrial gene order as a phylogenetic tool. Current Opinion in Genetics and Development. 1998; 8: 668–674. PMID: 9914213

84. Perseke M, Bernhard D, Fritzsch G, Brümmer F, Stadler PF, Schlegel M. Mitochondrial genome evolution in Ophiuroidea, Echinoidea, and Holothuroidea: insights in phylogenetic relationships of Echinodermata. Molecular Phylogenet Evolution. 2010; 56:201–211. https://doi.org/10.1016/j.ympev.2010.01.035 PMID: 20152912

85. Krylova EM, Sahling H. Recent bivalve molluscs of the genus *Calyptogena* (Vesicomyidae). Journal of Molluscan Studies. 2006; 72: 359–395. https://doi.org/10.1093/mollus/eyl022

86. Decker C, Olu K, Cunha RL, Arnaud-Haond S. Phylogeny and diversifcation patterns among vesicomyid bivalves. PLoS ONE. 2012; 7: e33359. https://doi.org/10.1371/journal.pone.0033359 PMID: 22511920

87. Johnson SB, Krylova EM, Audzijonyte A, Sahling H, Vrijenhoek RC. Phylogeny and origins of chemosynthetic vesicomyid clams. Systematics and Biodiversity. 2017; 15: 346–360. https://doi.org/10.1080/14772000.2016.1252438

88. Shen YY, Liang L, Zhu ZH, Zhou WP, Irwin DM, Zhang YP. Adaptive evolution of energy metabolism genes and the origin of flight in bats. Proceedings of the National Academy of Sciences of the United States of America. 2010; 107: 8666–8671. https://doi.org/10.1073/pnas.0912613107 PMID: 20421465

89. Tomasco IH, Lessa EP. The evolution of mitochondrial genomes in subterranean caviomorph rodents: adaptation against a background of purifying selection. Molecular Phylogenetics and Evolution. 2011; 61: 64–70. https://doi.org/10.1016/j.ympev.2011.06.014 PMID: 21723951

90. Plazzi F, Puccio G, Passamonti M. Burrowers from the past: mitochondrial signatures of Ordovician bivalve infaunalization. Genome Biology and Evolution. 2017; 9: 956–967. https://doi.org/10.1093/gbe/evx051 PMID: 28338965

91. da Fonseca RR, Johnson WE, O'Brien SJ, Ramos MJ, Antunes A. The adaptive evolution of the mammalian mitochondrial genome. BMC Genomics. 2008; 9: 119. https://doi.org/10.1186/1471-2164-9-119 PMID: 18318906

92. Yang YX, Xu SX, Xu JX, Guo Y, Yang G. Adaptive evolution of mitochondrial energy metabolism genes associated with increased energy demand in flying insects. Plos ONE. 2014; 9: e99120. https://doi.org/10.1371/journal.pone.0099120 PMID: 24918926

93. Das J. The role of mitochondrial respiration in physiological and evolutionary adaptation. BioEssays. 2006; 28: 890–901. https://doi.org/10.1002/bies.20463 PMID: 16937356

94. Zhang J, Nielsen R, Yang Z. Evaluation of an improved branch-site likelihood method for detecting positive selection at the molecular level. Molecular Biology and Evolution. 2005; 22: 247 2–2479. https://doi.org/10.1093/molbev/msi237 PMID: 16107592

95. Trumpower BL. The protonmotive Q cycle. Energy transduction by coupling of proton translocation to electron transfer by the cytochrome bc1 complex. Journal of Biological Chemistry. 1990; 265:11409–11412. PMID: 2164001

96. Silva G, Lima FP, Martel P, Caastilho R. Thermal adaptation and clinal mitochondrial DNA variation of European anchovy. Proceedings Biological Sciences. 2014; 281: 1792. https://doi.org/10.1098/rspb.2014.1093 PMID: 25143035

97. Luo YJ, Gao WX, Gao YQ, Tang S, Huang QY, Tan XL, et al. Mitochondrial genome analysis of *Ochotona curzoniae* and implication of cytochrome c oxidase in hypoxic adaptation. Mitochondrion. 2008; 8: 352–357. https://doi.org/10.1016/j.mito.2008.07.005 PMID: 18722554

98. Mahalingam S, McClelland GB, Scott GR. Evolved changes in the intracellular distribution and physiology of muscle mitochondria in high-altitude native deer mice. The Journal of Physiology. 2017; 595: 4785–4801. https://doi.org/10.1113/JP274130 PMID: 28418073

99. Chandel NS, Maltepe E, Goldwasser E, Mathieu CE, Simon MC, Schumacker PT. Mitochondrial reactive oxygen species trigger hypoxia-induced transcription. Proceedings of the National Academy of Sciences of the United States of America. 1998; 95: 11715–11720. https://doi.org/10.1073/pnas.95.20.11715 PMID: 9751731

100. Dirmeier R, O'Brien KM, Engle M, Dodd A, Spears E, Poyton RO. Exposure of yeast cells to anoxia induces transient oxidative stress. Implications for the induction of hypoxic genes. Journal of Biological Chemistry. 2002; 277: 34773–34784. https://doi.org/10.1074/jbc.M203902200 PMID: 12089150

101. Levin LA. Ecology of cold seep sediments: interactions of fauna with flow, chemistry and microbes. Oceanography and Marine Biology. 2005; 43:1–46.

102. Mu WD, Liu J, Zhang HB. Complete mitochondrial genome of *Benthodytes marianensis* (Holothuroidea: Elasipodida: Psychropotidae): Insight into deep sea adaptation in the sea cucumber. PLoS ONE. 2018; 13: e0208051. https://doi.org/10.1371/journal.pone.0208051 PMID: 30500836

103. Mu WD, Liu J, Zhang HB. The first complete mitochondrial genome of the Mariana Trench *Freyastera benthophila* (Asteroidea: Brisingida: Brisingidae) allows insights into the deep-sea adaptive evolution of Brisingida. Ecology and Evolution. 2018; 8: 10673–10686. https://doi.org/10.1002/ece3.4427 PMID: 30519397